

# Suzaku observation of an iron K-shell line in the spiral galaxy NGC 6946

Shigeo YAMAUCHI\*, Azusa INABA, and Yumiko ANRAKU

Faculty of Science, Nara Women's University, Kitaoyanishimachi, Nara, Nara 630-8506, Japan

\*E-mail: yamauchi@cc.nara-wu.ac.jp

Received ; Accepted

## Abstract

An emission line at  $\sim 6.7$  keV is attributable to a He-like iron K-shell transition, which indicates existence of a thin thermal plasma with a temperature of several keV. Using Suzaku archival data, we searched for the iron K-line from the spiral galaxy NGC 6946, and found the iron K-line at  $6.68 \pm 0.07$  keV at the  $3.1\sigma$  level in the central  $r \leq 2.5$  region. The iron line luminosity from the central region was estimated to be  $(2.3 \pm 1.2) \times 10^{37}$  erg s $^{-1}$  at a distance of 5.5 Mpc. The origin of the iron emission line is discussed.

**Key words:** galaxies: individual (NGC 6946) — X-rays: galaxies — X-rays: ISM

## 1 Introduction

Since the launch of the Einstein satellite with imaging capability, X-ray observations resolved individual X-ray sources and revealed the existence of diffuse X-ray emission with a temperature of  $< 1$  keV (e.g., Fabbiano 1989; Fabbiano et al. 1992; Read et al. 1997; Tyler et al. 2004; Owen & Warwick 2009; Mineo et al. 2012). The diffuse X-ray emission is thought to be X-rays from hot gas shock-heated by supernova (SN) explosions and stellar wind interactions.

An emission line at  $\sim 6.7$  keV is attributable to a K-transition line from He-like iron, which indicates existence of a thin thermal plasma with a temperature of several keV. The  $\sim 6.7$  keV emission line was detected from starburst galaxies (e.g., Pietsch et al. 2001; Boller et al. 2003; Strickland & Heckman 2007; Ranalli et al. 2008; Mitsuishi et al. 2011) and ultraluminous infrared galaxies (e.g., Iwasawa et al. 2005, 2009). The high temperature plasma was thought to be produced by multiple SNe after past starburst activities.

NGC 6946 is a face-on galaxy with four spiral arms. Its distance is estimated to be 5.5 Mpc (Tully 1988) – 7 Mpc (Israel 1980). NGC 6946 has strong nuclear star-

burst activity (e.g., Telesco & Harper 1980; Elmegreen et al. 1998), whereas further evidence for the high star forming activity, especially in the northern spiral arm, is indicated by CO radio emission line observations (e.g., Nietten et al. 1999; Walsh et al. 2002). The total star formation rate is estimated to be  $3.2 M_{\odot} \text{ yr}^{-1}$  (Jarrett et al. 2013). Active star formation in the past leads many SN explosions. In fact, 10 historical SNe have been observed since 1917 and a recent optical search for supernova remnants (SNRs) found many possible SNRs (Long et al. 2019).

X-ray observations of NGC 6946 have been carried out with Einstein, ROSAT, Chandra, and XMM-Newton and have revealed properties of X-ray emissions. In addition to discrete X-ray sources, a weak diffuse emission was detected (e.g., Schlegel 1994; Schlegel et al. 2003; Weźgowiec et al. 2016). Schlegel et al. (2003) estimated that as much as 10% of the total soft X-ray emission could be due to a diffuse component and showed that the diffuse component was explained by a two-component thermal plasma model with temperatures of  $0.25 \pm 0.03$  keV and  $0.70 \pm 0.10$  keV. Based on the XMM-Newton observation, Weźgowiec et al. (2016) revealed that parameters of the diffuse plasma exhibit spatial variation: two-temperature plasma models are needed for the disk and halo emission ( $kT_e \sim 0.2\text{--}0.3$  keV

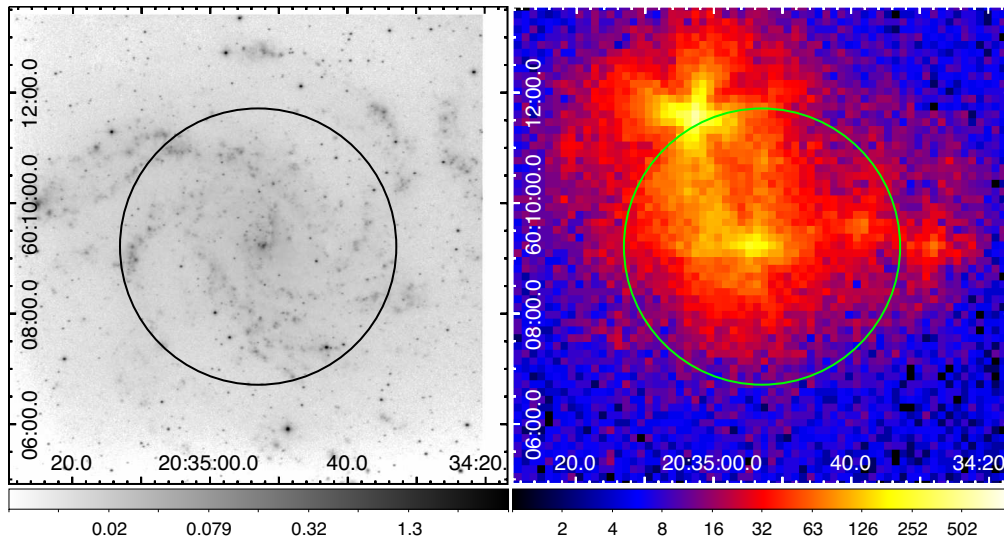


**Fig. 1.** NGC 6946  $H\alpha$  image taken from NASA/IPAC Extragalactic Database (<https://ned.ipac.caltech.edu>) (left) and XIS image in the 1–8 keV energy band (right). The coordinates are J2000.0. The intensity levels are logarithmically spaced. Data obtained with XIS 0, 1, and 3 sensors are merged. A solid circle shows a source region from which an X-ray spectrum was extracted.

and 0.6–0.8 keV), while the inter-arm regions show only one thermal component ( $kT_e \sim 0.4$ –0.6 keV). Weżgowiec et al. (2016) proposed that an increase of the temperature in the magnetic arm regions could be described as additional heating due to magnetic reconnection.

Is there a high temperature plasma having a 6.7 keV line in NGC 6946? Weżgowiec et al. (2016) did not state the existence of the iron K-line in the spectra. The detection of the iron K-line has not been reported so far. According to Snowden et al. (2008), the non X-ray background (NXB) of XMM-Newton is modeled as a power law function representing the soft proton contamination plus Gaussians representing instrumental fluorescence lines. The soft proton component has a hard spectrum extending up to  $\sim 12$  keV and is time-variable, which would affect estimation of a continuum shape and the iron K-line intensity of the diffuse component.

The X-ray Imaging Spectrometers (XIS, Koyama et al. 2007) onboard the Suzaku satellite (Mitsuda et al. 2007) has sufficient energy resolution and lower/more stable NXB than the previous X-ray satellites, and hence the XIS has the best sensitivity in the iron K-line band. Suzaku observed NGC 6946 with a long exposure time in a single observation ( $\sim 200$  ks), rather than several occasions as XMM-Newton. Therefore, the Suzaku XIS data is suitable to search for the iron K-line. In this paper, we present the results of a spectral analysis of NGC 6946 using the Suzaku XIS data and discuss the origin of the iron emission line. All through this paper, the errors are given as 90% confidence level.

## 2 Observation and data reduction

X-ray observation of NGC 6946 was made on 2012 May 13–16 with the Suzaku XIS (Koyama et al. 2007), which was placed on the focal planes of the thin foil X-ray Telescopes (XRT, Serlemitsos et al. 2007). The field of view (FOV) of the XIS was  $17'.8 \times 17'.8$ . The XIS was composed of 4 sensors: XIS sensor-1 (XIS 1) was a back-side illuminated CCD (BI), while the other three XIS sensors (XIS 0, 2, and 3) were front-side illuminated CCDs (FIs). However, one of the FIs (XIS 2) stopped working on 2006 November 9. Therefore, we utilized data obtained with three sensors, XIS 0, XIS 1, and XIS 3 for the following analysis. The XIS was operated in the normal clocking mode.

The Suzaku archival data were retrieved from the DARTS system operated by ISAS/JAXA. Data reduction and analysis were made using the HEASoft version 6.30.1 and the calibration database version 2018-10-10. The exposure time was 198.9 ks. In addition to the standard screening, we processed noisy pixel rejection according to the web page<sup>1</sup>.

## 3 Analysis and results

Figure 1 shows an  $H\alpha$  image and an XIS image in the 1–8 keV energy band. Several point-like X-ray sources are seen. The most luminous source located at the north-east from the center is identified with an ultra-luminous X-ray source, NGC 6946 X-1 (e.g., Fabbiano & Trinchieri

<sup>1</sup> <https://heasarc.gsfc.nasa.gov/docs/suzaku/analysis/xisnxbnew.html>

1987), associated with the optical nebula MF16 (Matonick & Fesen 1997). NGC 6946 X-1 exhibits a featureless spectrum (e.g., Roberts & Colbert 2003; Ghosh & Rana 2023), and it is thought to be a black hole binary. Results of a spectral analysis for NGC 6946 X-1 are presented in Appendix. In addition to the discrete sources, there seems to be a faint extended emission as is reported by Weżgowiec et al. (2016).

In order to examine existence of an iron K-line in NGC 6946, we carried out a spectral analysis. X-ray spectrum was extracted from a circle with a radius of  $2'.5$  (source region, a circle in figure 1). The NXB was taken from the night earth data using `xisnxbgen` (Tawa et al. 2008). After subtracting the NXB, we merged the FI spectra to maximize photon statistics. Response files, Redistribution Matrix Files (RMFs) and Ancillary Response Files (ARFs), were made using `xismfgen` and `xissimarfgen` (Ishisaki et al. 2007), respectively. In making the ARF, we assumed a uniform sky.

In order to maximize photon statistics, we added data with XIS 0 and 3 and grouped the data with a minimum of 40 counts per bin for XIS 0+3 and 20 counts per bin for XIS 1 after subtracting the NXB. The spatial resolution of the Suzaku XIS is worse than those of Chandra and XMM-Newton, and hence the source spectrum contains X-rays from not only diffuse X-ray emission but also discrete sources. In order to focus on searching for the iron K-line, we utilized the iron K-line band data.

Figure 2a shows the NXB-subtracted spectra in the 5–9 keV energy band. At first, we fitted the spectra with a bremsstrahlung + the Cosmic X-ray background (CXB) model modified by a low-energy absorption. The spectral parameters of the CXB were fixed to the values in Kushino et al. (2002), while the cross sections of the absorption were taken from Verner et al. (1996). As a result, we found positive residuals around 6.7 keV in the spectrum, as is shown in figure 2b. We added an emission line model with a line width of null to the spectra and found that the fit was improved (figure 2c). The  $\Delta\chi^2$  value was 10, which shows the F-test probability of 0.002. The significance level estimated from the obtained photon flux and its statistical error is  $3.1\sigma$ . The best-fitting parameters are listed in table 1 and the best-fitting model is plotted in figure 2a. After removing contribution of NGC 6946 X-1, an equivalent width was estimated to be  $0.19\pm 0.10$  keV.

The 6.7 keV emission line originates from a hot plasma with a temperature of several keV. We also examine the existence of 6.97 keV line attributable to a H-like iron K-shell transition. However, we found no obvious emission line and gave an upper limit of  $4.0\times 10^{-7}$  photons  $s^{-1}$   $cm^{-2}$  (90% confidence level).

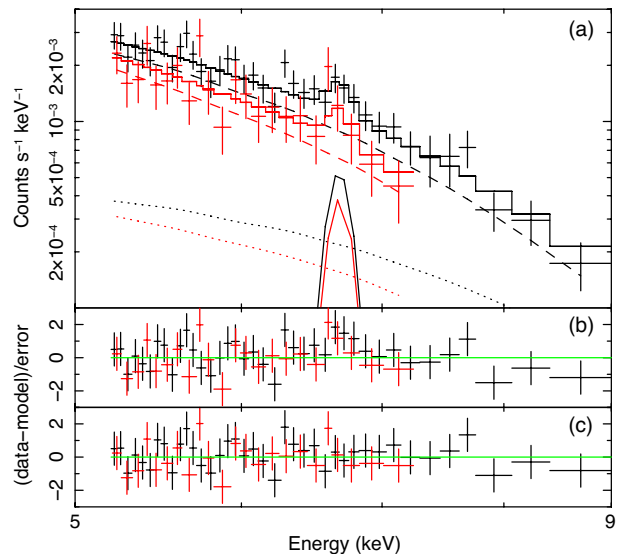


**Fig. 2.** (a) XIS spectra of the central region of NGC 6946 (black: XIS 0+3 and red: XIS 1) and the best-fitting model (histogram). The dashed, dotted, and the solid lines show contributions of continuum emission (thermal bremsstrahlung), the CXB, and an iron K-line, respectively. (b) Residuals from the best-fitting model without the iron K-line. (c) Residuals from the best-fitting model with the iron K-line.

**Table 1.** The best-fitting parameters of the central region.

Parameter	Value
Model:	phabs×(bremsstrahlung+line+CXB)
$N_H$ ( $cm^{-2}$ )	$2.2\times 10^{21}$ * (fixed)
$kT_e$ (keV)	$3.4^{+1.2}_{-0.7}$
$E_{Line}$ (keV)	$6.68\pm 0.07$
$I_{Line}$ (photons $s^{-1}$ $cm^{-2}$ )	$(5.9\pm 3.1)\times 10^{-7}$
Photon index <sub>CXB</sub>	1.412 (fixed)
Norm <sub>CXB</sub> <sup>†</sup>	$8.17\times 10^{-7}$ (fixed)
$\chi^2/d.o.f.$	42.4/58

\* HI4PI Collaboration: Ben Bekhti et al. (2016).

† In units of photons  $s^{-1}$   $cm^{-2}$   $arcmin^{-2}$  at 1 keV.

## 4 Discussion

Using the Suzaku data, we detected an iron K-line at  $6.68\pm 0.07$  keV with a  $3.1\sigma$  level. The previous work using XMM-Newton (Weżgowiec et al. 2016) did not report whether the iron K-line was found in the spectra or not. Thus, we analyzed the XMM-Newton archival data (7 occasions, total accumulated time= $229.9$ ,  $232.7$ , and  $177.9$  ks for MOS1, MOS2, and pn, respectively) and examined whether the iron K-line can be seen. We fitted the spectra extracted from a central  $r \leq 2'.5$  region (same as that of the Suzaku data analysis) with the same spectral model as that in the Suzaku observation and found a hint of the iron K-line at 6.68 keV. The line flux was estimated to be

$(7.3 \pm 3.0) \times 10^{-7}$  photons  $\text{s}^{-1} \text{cm}^{-2}$  ( $4.0 \sigma$  level), consistent with that in the Suzaku observation.

Using the best-fitting parameters for the Suzaku spectrum, we calculated the iron line luminosity to be  $L_{\text{Fe}} = (2.3 \pm 1.2) \times 10^{37}$  erg  $\text{s}^{-1}$  within a  $2.5$  radius, a  $4$  kpc radius at a distance of  $5.5$  Mpc (Tully 1988). Schlegel et al. (2003) and Weżgowiec et al. (2016) reported the existence of a hot plasma with a temperature of  $\sim 0.7$ – $0.8$  keV. The iron line centroid is less than  $6.6$  keV in the  $0.7$ – $0.8$  keV plasma. Since the lower end of the observed line centroid is  $6.61$  keV, we can safely conclude that NGC 6946 has a hotter plasma than those found by Schlegel et al. (2003) and Weżgowiec et al. (2016). Following argument in M101 paper (Yamauchi 2016), we discuss the origin of the iron emission line.

Stellar sources such as cataclysmic variables (CVs), active binaries (ABs), and young stellar objects (YSOs) in star forming regions are known to have a thin thermal emission with the iron emission line (e.g., Ezuka & Ishida 1999; Güdel et al. 1999; Yamauchi et al. 1996). At first, we discuss the stellar source origin.

Sazonov et al. (2006) showed a cumulative luminosity density of the stellar sources in the Galaxy to be  $L_{\star, 2-10\text{keV}}/M_{\star} = (4.5 \pm 0.9) \times 10^{27}$  erg  $\text{s}^{-1} M_{\odot}^{-1}$ , where  $L_{\star, 2-10\text{keV}}$  is a stellar source luminosity in the  $2$ – $10$  keV band and  $M_{\star}$  is a stellar mass. Assuming the typical spectral model for CVs, ABs, and YSOs (e.g., Baskill et al. 2005; Ishida et al. 2009; Güdel et al. 1999; Yamauchi et al. 1996), we can estimate a stellar source iron line luminosity,  $L_{\star, \text{Fe}}$ , to be  $3$ – $4\%$  of  $L_{\star, 2-10\text{keV}}$ . The rotation velocity of NGC 6946 of  $\sim 170$  km  $\text{s}^{-1}$  at the radius of  $4$  kpc (de Blok et al. 2008) gives the total mass within the central  $4$  kpc radius region of  $2.7 \times 10^{10} M_{\odot}$ . This value is an upper limit of the stellar mass because galaxies contains interstellar matter, high mass stars, X-ray sources such as black hole binaries and neutron-star binaries, a supermassive black hole at the center, and dark mater as well as CVs, ABs, and YSOs. Assuming all the mass is equal to the total mass of CVs, ABs, and YSOs, we obtain  $L_{\star, 2-10\text{keV}} = (0.9$ – $1.5) \times 10^{38}$  erg  $\text{s}^{-1}$ , and then  $L_{\star, \text{Fe}} \leq 6 \times 10^{36}$  erg  $\text{s}^{-1}$ . Thus, the well-known stellar sources cannot account for all the observed  $L_{\text{Fe}}$ . Taking account of contribution of the stellar sources, we can conclude that  $L_{\text{Fe}} \sim 10^{37}$  erg  $\text{s}^{-1}$  originates from other objects or process.

Young and middle-aged SNRs have a several keV temperature plasma and exhibit an intense iron K line. Thus, hot plasmas produced by SN explosions are a possible candidate. The typical SNR luminosity of  $L_{\text{SNR}, 2-10\text{keV}} \sim 10^{34-36}$  erg  $\text{s}^{-1}$  (e.g., Seward 2000). Assuming a several keV temperature and solar abundances (Anders & Grevesse 1989), we can estimate  $L_{\text{SNR}, \text{Fe}}$  to be

$\sim 7\%$  of  $L_{\text{SNR}, 2-10\text{keV}}$ , and hence  $L_{\text{SNR}, \text{Fe}}$  of each SNR to be  $\sim 10^{33-35}$  erg  $\text{s}^{-1}$ . The total number of SNRs,  $N_{\text{SNR}}$  to account for the  $L_{\text{Fe}} \sim 10^{37}$  erg  $\text{s}^{-1}$  is  $\sim 100$ – $10^4$ . According to the Sedov solution (Sedov 1959), a typical SNR age with a temperature of  $> 1$  keV ( $t$ ) is  $\leq 4 \times 10^3$  yr. Thus, a SN rate to explain the observed  $L_{\text{Fe}}$  is  $N_{\text{SNR}}/t \sim 0.03$ – $3$  yr $^{-1}$  within the  $4$  kpc radius. The SN rate is estimated to be  $\sim 0.1$  yr $^{-1}$  based on the fact that  $10$  SNe have been discovered since 1917. Multiple SN explosions following the active star formation can produce a large amount of diffuse hot plasma.

Since many SNRs and SNR candidates were discovered in the whole galaxy (Long et al. 2019), SNe in the Galactic arm would contribute to producing the diffuse hot plasma considerably. The image obtained with XMM-Newton showed a diffuse emission around the central region of NGC 6946 as well as along the Galactic arm (Weżgowiec et al. 2016). The  $6.7$  keV line enhancement was found in the central region of the starburst galaxy NGC 253 (Mitsuishi et al. 2011). Substantial iron line emission may associate with the activity in the central region such as a nuclear starburst.

Schlegel et al. (2003) and Weżgowiec et al. (2016) reported existence of a hot plasma with a temperature of  $\sim 0.7$ – $0.8$  keV in NGC 6946 and slightly enhancement of the temperature in the arm regions. Weżgowiec et al. (2016) estimated the magnetic field strength to be  $\sim 10$ – $20$   $\mu\text{G}$  and proposed magnetic reconnection as additional heating. As a scenario of the Galactic Ridge X-ray Emission (GRXE), which is distributed along the Galactic plane and exhibits an intense iron K-line (e.g., Koyama 2018), Tanuma et al. (1999) showed that the magnetic reconnection heats a cool ( $\sim 0.8$  keV) plasma generated by SNe up to the hot ( $\sim 7$  keV) plasma, if the local magnetic field strength is  $\sim 30$   $\mu\text{G}$  with a filling factor of  $< 0.1$ . Here, we discuss on possibility of the magnetic activity based on the present results.

Adopting a temperature of  $3$  keV from the spectral fitting (see table 1) and solar abundance for the hot plasma and  $L_{\text{Fe}} \sim 10^{37}$  erg  $\text{s}^{-1}$  within a  $2.5$  radius, we estimated the luminosity in the  $2$ – $10$  keV band to be  $\sim 10^{38}$  erg  $\text{s}^{-1}$ . Assuming the X-ray emitting volume of a cylinder with a radius of  $4$  kpc and a height of  $400$  pc and  $n_e = 1.2n_H$ , where  $n_e$  and  $n_H$  are electron and hydrogen densities, respectively, we obtained  $n_H$  of  $\sim 5 \times 10^{-3} f^{-0.5}$  cm $^{-3}$  and a thermal energy density of  $\sim 7 \times 10^{-11} f^{-0.5}$  erg cm $^{-3}$ , where  $f$  is a filling factor. Since the total thermal energy is larger than the energy density of magnetic field of  $(0.7$ – $1.9) \times 10^{-11}$  erg cm $^{-3}$  (Weżgowiec et al. 2016), it is difficult to account for all the hot plasma by only the magnetic energy.

Using XMM-Newton data of M101, Weżgowiec et al. (2022) argued what amount of the magnetic energy density would be converted to thermal energy by the magnetic reconnection and consequently increase the temperature of the hot gas. In their estimation, a magnetic energy density of  $\sim 2 \times 10^{-13}$  erg cm $^{-3}$ , which is about 10% of the total magnetic energy density, would be converted to additional thermal energy of  $\sim 10^{-10}$  erg per particle in the hot gas having a density of  $\sim 10^{-3}$  cm $^{-3}$ , which leads to an increase in temperature by around 0.1 keV. Applying the same estimation to the case of NGC 6946, we found that the total magnetic energy density of  $\sim (1-2) \times 10^{-11}$  erg cm $^{-3}$  is enough to add a thermal energy of  $\sim 10^{-10}$  erg per particle in the hot gas. Thus, additional heating for primary hot plasma, probably produced by SNe, by the magnetic reconnection would be possible.

A hot plasma with a temperature of a few keV cannot be bound by the galactic gravity and it would cool down once the reconnection stops to operate. Therefore, if this process works, continuous heating by reconnection and some processes to maintain the hot plasma such as magnetic confinement proposed by Makishima (1994) should be required. To investigate this process in detail, we need to know spatial distribution and physical parameters (temperature, density, thermal energy, and so on) of the hot plasma after removing contribution of point sources.

Masai et al. (2002) proposed a scenario of the origin of the GRXE based on stochastic particle acceleration in the interstellar medium. Free electrons in the hot interstellar medium produced by SNe are scattered and accelerated through a stochastic process by irregular magnetic fields left behind SNR shocks. The electron spectrum is reproduced approximately by the sum of the a few hundred eV Maxwellian of thermal electrons produced by SNe, power-law non-thermal component, and a few keV Maxwellian of quasi-thermal electrons. A thermal plasma at a few hundred eV can be bound by the galactic gravity. Highly ionized iron is produced by ionization by the quasi-thermal electrons. In addition, a fraction of ions also captures background thermal electrons, i.e., recombining. Thus, in the case of this model, the iron K-line and many recombination edges on the non-equilibrium continuum spectrum, especially recombination structure by iron ion at 8–9 keV, can be seen in the spectrum. However, we see no recombination structure in the Suzaku spectrum due to limited photon statistics.

## 5 Conclusion

Using Suzaku archival data, we detected the iron K-line at 6.68 keV at the  $3.1\sigma$  level in the central  $r \leq 2.5$  region of

NGC 6946 for the first time. The iron line luminosity from the central region was estimated to be  $(2.3 \pm 1.2) \times 10^{37}$  erg s $^{-1}$  at a distance of 5.5 Mpc. Contribution of stellar sources in NGC 6946 is not enough to explain the total iron K-line luminosity, and hence  $L_{\text{Fe}} \sim 10^{37}$  erg s $^{-1}$  originates from other objects or process. SNe with a high SN rate are considered to be a possible scenario. The magnetic energy density is not enough to account for all the hot plasma with the iron K-line, but additional heating for primary hot plasma by the magnetic reconnection would be possible. A quasi-thermal electrons produced by a stochastic acceleration may be the origin of the iron K-line. Unfortunately, due to limited spatial resolution and photon statistics of the Suzaku observation, we cannot conclude which process works. We need further observations with high spatial resolution and good photon statistics to reveal the origin of the emission line.

## Acknowledgements

The authors are grateful to all members of the Suzaku team. The authors wish to thank the referee for constructive comments that improved the manuscript. This work was supported by the Japan Society for the Promotion of Science (JSPS) KAKENHI Grant Numbers JP 21K03615 (SY).

## Appendix: X-ray spectrum of NGC 6946 X-1

The source spectrum was extracted from a  $40''$  radius circle. The background spectrum was extracted from an annulus with inner and outer radii of  $60''$  and  $90''$ , respectively, but excluding the source region. We added data with XIS 0 and 3 and grouped the data with a minimum of 50 counts per bin for both XIS 0+3 and XIS 1 spectra. The ARF was made as a point source at the position of NGC 6946 X-1. The background-subtracted source spectra are shown in figure 3. We fitted the spectrum with model consisting of a multi-color disk (`diskbb` model in XSPEC, Mitsuda et al. 1984) and a thermally Comptonized continuum (`thcomp` model in XSPEC, Zdziarski et al. 2020) modified by a low energy absorption (`phabs` model in XSPEC) but found that the model showed a systematic broad residuals around 1 keV. Referring Ghosh & Rana (2023), we added a broad Gaussian at 0.9 keV and obtained an improved fit. The best-fitting parameters are listed in table 2, while the best-fitting model is plotted in figure 3. The luminosity was estimated to be  $\sim 2 \times 10^{39}$  erg s $^{-1}$  in the 2–10 keV band at 5.5 Mpc. We found no significant line at 6.7 keV ( $< 7 \times 10^{-7}$  photons s $^{-1}$  cm $^{-2}$ , 90 % confidence level).

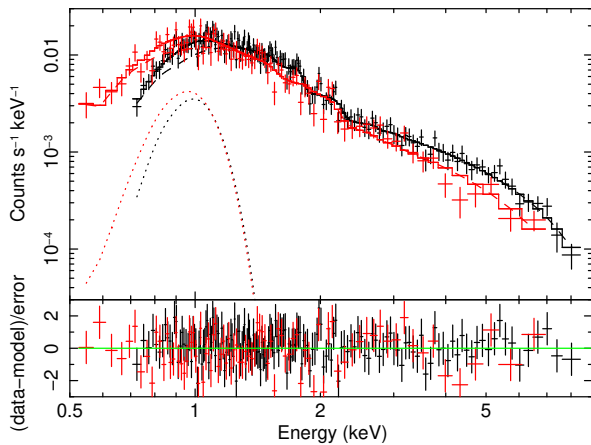


**Fig. 3.** Upper panel: XIS spectra of NGC 6946 X-1 (black: XIS 0+3 and red: XIS 1) and the best-fitting model (histogram). The dashed and dotted lines show continuum emission and a broad Gaussian, respectively. Lower panel: Residuals from the best-fitting model.

**Table 2.** The best-fitting parameters of NGC 6946 X-1.

Parameter	Value
Model: $\text{phabs} \times (\text{thcomp} \times \text{diskbb} + \text{gaussian})$	
$N_{\text{H}}$ ( $\text{cm}^{-2}$ )	$2.2 \times 10^{21}$ * (fixed)
$kT_{\text{in}}$ (keV)	$0.23^{+0.08}_{-0.05}$
Norm	$19^{+34}_{-15}$
Photon index	$2.3 \pm 0.2$
$kT_e$ (keV)	100 (fixed)
Covering fraction	$> 0.53$
$E_{\text{Gaussian}}$ (keV)	$0.90^{+0.07}_{-0.12}$
$\sigma_{\text{Gaussian}}$ (keV)	$0.14^{+0.07}_{-0.05}$
$I_{\text{Gaussian}}$ ( $\text{photons s}^{-1} \text{cm}^{-2}$ )	$(6.0^{+9.8}_{-3.0}) \times 10^{-5}$
$\chi^2/\text{d.o.f.}$	236.1/239

\* HI4PI Collaboration: Ben Bekhti et al. (2016).

## References

Anders, E., & Grevesse, N. 1989, *Geochim. Cosmochim. Acta*, 53, 197

Baskill, D. S., Wheatley, P. J., & Osborne, J. P. 2005, *MNRAS*, 357, 626

Boller, T., et al. 2003, *A&A*, 411, 63

de Blok, W. J. G., Walter, F., Brinks, E., Trachternach, C., Oh, S.-H., & Kennicutt, R. C., Jr. 2008, *AJ*, 136, 2648

Elmegreen, D. M., Chromey, F. R., & Santos, M. 1998, *AJ*, 116, 1221

Ezuka, H., & Ishida, M. 1999, *ApJS*, 120, 277

Fabbiano, G. 1989, *ARA&A*, 27, 87

Fabbiano, G., & Trinchieri, G. 1987, *ApJ*, 315, 46

Fabbiano, G., Kim, D.-W., & Trinchieri, G. 1992, *ApJS*, 80, 531

Ghosh, T., & Rana, V. 2023, *ApJ*, 949, 78

Güdel, M., Linsky, J. L., Brown, A., & Nagase, F. 1999, *ApJ*, 511, 405

HI4PI Collaboration: Ben Bekhti, N., et al. 2016, *A&A*, 594, A116

Ishida, M., Okada, S., Hayashi, T., Nakamura, R., Terada, Y., Mukai, K., & Hamaguchi, K. 2009, *PASJ*, 61, S77

Ishisaki, Y., et al. 2007, *PASJ*, 59, 113

Israel, P. F. 1980, *A&A*, 90, 246

Iwasawa, K., Sanders, D. B., Evans, A. S., Mazzarella, J. M., Armus, L., & Surace, J. A. 2009, *ApJ*, 695, L103

Iwasawa, K., Sanders, D. B., Evans, A. S., Trentham, N., Miniutti, G., & Spoon, H. W. W. 2005, *MNRAS*, 357, 565

Jarrett, T. H., et al. 2013, *AJ*, 145, 6

Koyama, K. 2018, *PASJ*, 70, 1

Koyama, K., et al. 2007, *PASJ*, 59, S23

Kushino, A., Ishisaki, Y., Morita, U., Yamasaki, N. Y., Ishida, M., Ohashi, T., & Ueda, Y. 2002, *PASJ*, 54, 327

Long, K. S., Winkler, P. F., & Blair, W. P. 2019, *ApJ*, 875, 85

Makishima, K. 1994, in *New Horizon of X-Ray Astronomy, First Results from ASCA*, ed. F. Makino & T. Ohashi (Tokyo: Universal Academy Press), 171

Masai, K., Dogiel, V. A., Inoue, H., Schönfelder, V., & Strong, A. W. 2002, *ApJ*, 581, 1071

Matonick, D. M., & Fesen, R. A. 1997, *ApJS*, 112, 49

Mineo, S., Gilfanov, M., & Sunyaev, R. 2012, *MNRAS*, 426, 1870

Mitsuda, K., et al. 1984, *PASJ*, 36, 741

Mitsuda, K., et al. 2007, *PASJ*, 59, S1

Mitsuishi, I., Yamasaki, N. Y., & Takei, Y. 2011, *ApJ*, 742, L31

Nieten, C., Dumke, M., Beck, R., & Wielebinski, R. 1999, *A&A*, 347, L5

Owen, R. A., & Warwick, R. S. 2009, *MNRAS*, 394, 1741

Pietsch, W., et al. 2001, *A&A*, 365, L174

Ranalli, P., Comastri, A., Origlia, L., & Maiolino, R. 2008, *MNRAS*, 386, 1464

Read, A. M., Ponman, T. J., & Strickland, D. K. 1997, *MNRAS*, 286, 626

Roberts, T. P., & Colbert, E. J. M. 2003, *MNRAS*, 341, L49

Sazonov, S., Revnivtsev, M., Gilfanov, M., Churazov, E., & Sunyaev, R. 2006, *A&A*, 450, 117

Schlegel, E. M. 1994, *ApJ*, 434, 523

Schlegel, E. M., Holt, S. S., & Petre, R. 2003, *ApJ*, 598, 982

Sedov, L. I. 1959, *Similarity and dimensional method in mechanics*, 10th ed. (New York: Academic Press)

Serlemitsos, P., et al. 2007, *PASJ*, 59, S9

Seward, F. D. 2000, in *Allen's Astrophysical Quantities*, 4th ed., ed. A. N. Cox (New York, Springer), Chapter 9

Snowden, S. L., Mushotzky, R. F., Kuntz, K. D., & Davis, D. S. 2008, *A&A*, 478, 615

Strickland, D. V., & Heckman, T. M. 2007, *ApJ*, 658, 258

Tanuma, S., et al. 1999, *PASJ*, 51, 161

Tawa, N., et al. 2008, *PASJ*, 60, S11

Telesco, C. M., & D. A. Harper, D. A. 1980, *ApJ*, 235, 392

Tully, R. 1988, *Nearby Galaxies Catalog* (Cambridge: Cambridge Univ. Press)

Tyler, K., Quillen, A. C., LaPage, A., & Rieke, G. H. 2004, *ApJ*, 610, 213

Verner, D. A., Ferland, G. J., Karista, K. T., & Yakovlev, D. G. 1996, *ApJ*, 465, 487

- Walsh, W., Beck, R., Thuma, G., Weiss, A., Wielebinski, R., & Dumke, M. 2002, *A&A*, 388, 7
- Weźgowiec, M., Ehle, M., & Beck, R. 2016, *A&A*, 585, A3
- Weźgowiec, M., Beck, R., Hanasz, M., Soida, M., Ehle, M., Dettmar, R. -J., & Urbanik, M. 2022, *A&A*, 664, A108
- Yamauchi, S., Koyama, K., Sakano, M., & Okada, K. 1996, *PASJ*, 48, 719
- Yamauchi, S. 2016, *PASJ*, 68, S18
- Zdziarski, A. A., Szanecki, M., Poutanen, J., Gierliński, M., & Biernacki, P. 2020, *MNRAS*, 492, 5234